2010 IEEE International Conference on Robotics and Automation
Anchorage Convention District
May 3-8, 2010, Anchorage, Alaska, USA

Training Special Needs Infants to Drive Mobile Robots Using Force-Feedback Joystick

Sunil K. Agrawal, Xi Chen, and James C. Galloway

Abstract— **In typically developing infants, the onset of crawling and walking is associated with changes across development domains such as cognition and perception ([1], [2]). Currently, infants born with significant mobility impairments do not use powered wheelchairs until three years of age [3]. This potentially limits their development in the early growth years. The goal of this research is to train infants with impairments to safely and purposefully drive a mobile robot indoors while being seated on it. We anticipate that these impaired infants will benefit from early mobility in their early years, similar to their healthy peers.**

Our studies with 3-12 month old infants have shown that in about six weeks of training on the mobile robot, infants can learn to drive purposefully using conventional joysticks [4]. However, they are unable to directionally control the mobile robot [5]. This poses limits on how infants can drive independently within a home environment.

This paper is the first to show novel results where special needs infants learn how to make sharp turns during driving, when trained over a 5-day period with a force-feedback joystick. The joystick simulates a virtual tunnel around an intended path with turns. During training, if the infant driver moves the mobile robot outside this tunnel centered around the desired path, the driver experiences a bias corrective force on the hand. This ***assist-as-needed*** **paradigm may be suitable for infant driving training and has worked well in other studies on functional training of human movements [6].**

I. INTRODUCTION

Today, haptic device is becoming a powerful tool to augment virtual reality. Force-feedback joysticks are used to improve device control of humans and provide assistance in performing tasks ([8], [9], [10], [9], [11], [12], [13], [14]). The goal of this paper is different and novel, i.e., to train special needs infants, under 3 years of age, to drive independently and make purposeful turns with a vehicle using a force-feedback joystick. *Currently, there is no research that attempts to train very young infants to drive mobile robots using joysticks, while they are seated on it.*

Today, mobile robots can be made to autonomously follow commanded paths using onboard sensors and available error correcting control strategies. *However, the question that we ask in this paper is if special needs infant drivers under 3 years of age can learn these error correcting strategies through training, using force-feedback joysticks?* Some recent studies in gait rehabilitation of healthy and stroke patients have shown that humans learn to improve walking if they are trained using force tunnels around desired foot paths ([7], [6]).

Sunil K. Agrawal is a Professor of Mechanical Engineering at the University of Delaware, Newark, DE 19716. He is also the Corresponding Author.

Xi Chen is a PhD student in the Department of Mechanical Engineering, University of Delaware, Newark, DE 19716.

James C. Galloway is an Associate Professor of Physical Therapy at the University of Delaware, Newark, DE 19716.

This research is supported by grants from National Science Foundation and National Institute of Health.

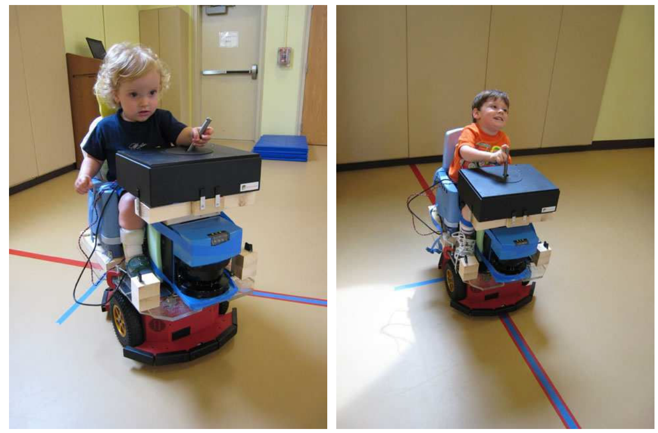

Fig. 1. Directional Training experiments using force feedback joystick on two infants diagnosed with spina bifida and cerebral palsy.

With this goal and strategy in mind, the rest of this paper is organized as follows: Section II describes the experiment setup and the nature of force field applied to train infant drivers. Before conducting experiments with infants, we recruited adult subjects to assess the usefulness of force feedback joystick on human training. This is described in Section III. Training results of two developmentally delayed infants with spina-bifida and cerebral palsy are provided in Section IV.

II. EXPERIMENT SETUP AND TRAINING ALGORITHM

A. Training Hardware

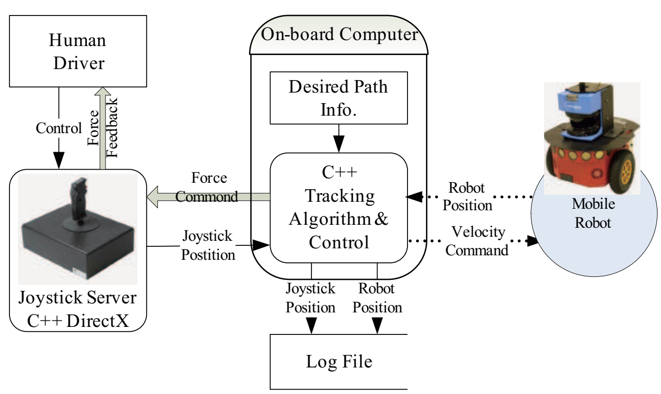

Fig. 2. A schematic of the experimental setup, its components, and data flow from and to an infant driver.

Fig. 1 shows two infant drivers who underwent training with an in-house assembled experiment setup consisting of a mobile robot, sensors, and a force-feedback joystick. Fig. 2 shows the schematics of various modules of the experiment test-bed. The force feedback joystick is an Immersion Impulse Stick® that can provide continuous force of 8.5N and peak force of 14.5N. The joystick interface is through DirectX®, which can read joystick position and applies forces on the hand. The mobile robot is a differentially driven 2-wheel Pioneer 3-DX robot® equipped with encoders to record trajectory. A user develops programs to determine speed commands to the vehicle and joystick forces. These programs interface with an on-board library which has access to current position, orientation of the robot, obstacle free area around it, and infant's joystick inputs.

B. Training Path and Wall Following Strategy

The training path, shown in Fig. 3, is chosen to consist of three straight lines interspersed with a right and a left turn. A robot could autonomously follow this path using the wall following strategy described below. *The research challenge is if a special needs infant driver will learn such a wall following strategy, when assisted by the force feedback joystick.*

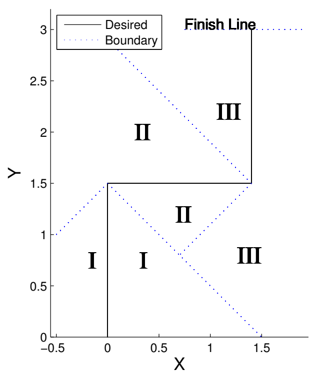

Fig. 3. The training path consists of three black lines, driving in straight line, a right turn and a left turn.

Fig. 4(i) shows the schematic of a robot with the goal to follow a wall inclined at φ from the horizontal. The kinematic model of a differentially driven mobile robot has the following form:

$$\begin{cases} \dot{x}_c = v\cos\theta \\ \dot{y}_c = v\sin\theta \\ \dot{\theta} = \omega. \end{cases} \tag{1}$$

Here, x_c and y_c are coordinates of the robot center and θ is its orientation. d is the normal distance between the robot center and the inclined path. The inputs to the robot are the translational speed v and rotational speed ω. In the figure, the current heading of the robot is shown at an angle $\Delta\theta$ from the wall. A wall following algorithm, such as [15], is an error correcting control law that specifies the inputs v and ω such that $d \to 0$ and $\Delta\theta \to 0$ as time increases. This control law is given by

$$\begin{cases} v = v_{des} \\ \omega = -\frac{k_1 d}{v_{des}\cos\Delta\theta} - k_2 \tan\Delta\theta \end{cases} . \tag{2}$$

We divide the training area into three regions: I, II, and III (Fig. 3). The robot will switch to track the next line if it is inside the corresponding region. Fig. 4(ii) shows simulation of a path when such a strategy is applied autonomously to the mobile robot.

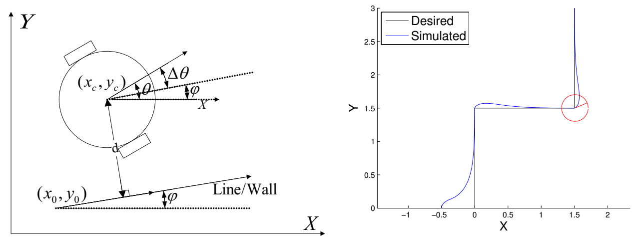

Fig. 4. (i) Schematic of a robot intended to follow a straight path inclined at an angle φ, (ii) Simulation of the robot trajectory using an autonomous wall following algorithm. Initial condition: $(x, y, \theta) = (-0.5, 0, \pi/2)$

C. Nominal Joystick Motion and Force Tunnels

v and ω computed using the wall following strategy can be viewed as ideal commands for an autonomously driven robot. However, in experiments, the speed commands are given by the infant driver through the joystick. Hence, v and ω commands need to be mapped on to the motion of the joystick. A joystick has predominantly two motions - forward/backward and left/right. We map pure forward/backward motion of the joystick to forward/backward motion of the vehicle along the heading direction. The pure side to side motion of the joystick is mapped to pure rotation of the vehicle. In practice, we scale forward/backward joystick position using $\text{Max\_V} = 0.24$ meters/second and side to side joystick position using $\text{Max\_W} = 30°/\text{second}$. Hence, given the desired control input v_{des} and ω, the ideal joystick movement direction is mapped to

$$\beta = \text{Atan2}\left(\frac{v_{des}}{\text{Max\_V}}, \frac{\omega}{\text{Max\_W}}\right) \tag{3}$$

where Atan2(.,.) is a 2-argument 'arctan' function.

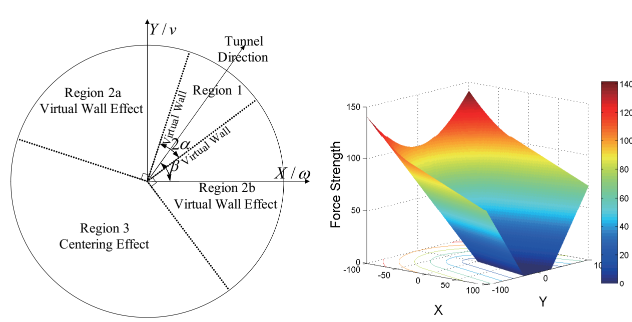

Fig. 5. (i) Force Tunnel shown by a virtual walls around Nominal Joystick Motion Direction, (ii) Tip force within the cone is zero. Tip force outside the cone for the tunnel direction $\beta = 0$ and half tunnel width $\alpha = 15°$. The damping effect not shown in these plots.

The force tunnel is depicted by a cone of angle 2α around the nominal direction of joystick motion β. In the 'assist-as-needed' paradigm for training, no force field is applied on the hand, if the driver initiates a joystick motion within the cone. Fig. 5(i) shows graphically four regions around this instantaneous direction of motion.

We define three force effects which qualitatively are:

1) *centering effect* - applies a restoring force to bring the handle of the joystick back to the center. It can be represented as
$$\mathbf{F}_c = -k_c\mathbf{p} \tag{4}$$
where $\mathbf{p} = [x_l, y_l]^T$ is the joystick handle position. In real programming using DirectX, the coefficient k_c is selected so that when $\mathbf{p}$ reaches its max value, $k_c\mathbf{p}$ will be the max allowable force input in DirectX.
2) *virtual wall effect* - applies a restoring force to bring the handle of the joystick back to region A. This force is normal to the virtual wall and proportional to the distance from the wall. The unit vector along the virtual wall between Region 1 and Region 2a/2b is
$$\mathbf{w} = [\cos(\beta \pm \alpha),\ \sin(\beta \pm \alpha)]^T \tag{5}$$
The virtual wall effect can be represented by
$$\mathbf{F}_w = k_c[(\mathbf{p}\cdot\mathbf{w})\mathbf{w} - \mathbf{p}] \tag{6}$$
3) *damping effect* - applies force on the tip of the joystick in a direction opposite to its displacement. This force prevents chattering of the joystick. Mathematically,
$$\mathbf{F}_d = -k_d[\dot{x}_l, \dot{y}_l]^T \tag{7}$$
where $\dot{x}_l, \dot{y}_l$ are the joystick tip speeds in the joystick frame. The coefficient k_d is selected to be the minimal value so that the joystick handle does not vibrate.

The haptic forces in the four regions of Fig. 5 are as follows:

1) Region 1: Damping effect to stabilize the joystick. $\mathbf{F} = \mathbf{F}_d$
2) Region 2a & 2b: Vector sum of virtual wall and damping effects. $\mathbf{F} = \mathbf{F}_w + \mathbf{F}_d$.
3) Region 3: Vector sum of centering and damping effect. $\mathbf{F} = \mathbf{F}_c + \mathbf{F}_d$.

A haptic force field, with the above choice, is shown in Fig. 5(ii). The z-coordinate represents the force magnitude. The x-y plane represents the joystick workspace. Note this force field function is continuous.

III. Adult Driving Experiments

Before conducting experiments with infants, we recruited eight adult subjects to assess the usefulness of force feedback joystick on human training. These eight subjects were divided into two groups: training group and control group. All subjects were healthy adults ranging from 25 to 30 years.

The subjects use the joystick to remotely control the mobile robot to track the given path, see Fig. 6. The training group uses the force feedback from the joystick while the control group does not. The objective of this experiment is not only to test whether this force field can help human drive more accurately but also to see if this force field results in learning. *The learning is tested by pre and post training evaluation experiments in the absence of force field.*

Fig. 6. Training experiments with healthy subjects

The training protocol is designed as follows: Each training consists of four sessions. During each session, there are 5 trials. Subjects are asked to follow the lines as accurately as possible.

1) Session 1 (Pre-training): This serves to collect the base line data of the subject. No force feedback is given to either group.
2) Session 2 (Training 1): The force field is turned on for the training group.
3) Session 3 (Training 2): The force field is turned on for the training group.
4) Session 4 (Post-training): No force feedback is given to either group. The data from this session is compared to those collected in the Pre-training to determine learning.

The data on robot position and total travel time are recorded and used for comparisons. We calculate the deviation from the desired path by the area shown in Fig. 7. This area is obtained by numerical integration and uses the average of the 5 trials to represent the results of a session. We also calculate the average time of each session.

A. Results

The experiment results are listed in Tables I-IV. Note that the *decrease* column is calculated as $-\frac{post-pre}{pre}$ to measure the improvement after the training. From the data presented in Tables I-IV, we can make the following observations:

TABLE I
Training Group: Deviation Area (m^2)

Subject	Pre	T 1	T 2	Post	Decrease
1	0.1270	0.0711	0.0665	0.0685	46.10%
2	0.2287	0.1979	0.1581	0.1930	15.61%
3	0.2002	0.1661	0.1635	0.1713	14.42%
4	0.2349	0.2159	0.1613	0.1669	28.98%

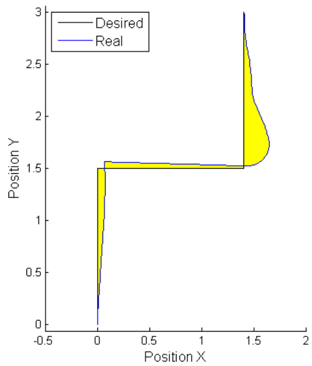

Fig. 7. An illustration of the deviation from the desired path, shown in yellow

TABLE II

TRAINING GROUP: TRAVEL TIME (*second*)

Subject	Pre	T 1	T 2	Post
1	24.13	27.59	26.10	25.71
2	30.58	35.44	32.33	31.57
3	38.60	34.55	34.80	33.76
4	27.80	29.94	28.88	31.18

1) The tunnel force field provides learning to the driver. The performance of all subjects in the training group improves, illustrated by comparison of data between the Pre- and Post-training (paired t-test, $p = 0.015$). However, the performance of subjects in the control group does not show improvements (Paired t-test, $p = 0.76$). Hence, we believe that the performance increase of the training group is due to force feedback training (See Fig. 8).
2) With force feedback turned on, the subjects track the path better, as shown in Figs. 9 and 8. Both results in Training 1 and 2 are better than Pre-training (paired t-test on Pre- and Training 1, $p = 0.021$). The results of Training 2 are better, though not significantly, than Post-training (paired t-test, $p = 0.194$), indicating that subjects performed much better after the training sessions.
3) We did not observe any special pattern from the time of completion data. The subjects maintain a consistent travel time which does not change much during the 4 sessions.

TABLE III

CONTROL GROUP: DEVIATION AREA (m^2)

Subject	Pre	T 1	T 2	Post	Decrease
5	0.1393	0.2017	0.2082	0.2178	-56.40%
6	0.1503	0.1797	0.1915	0.1742	-15.89%
7	0.2343	0.2528	0.1744	0.2388	-1.93%
8	0.2256	0.1683	0.1784	0.1592	29.46%

TABLE IV

CONTROL GROUP: TRAVEL TIME (*second*)

Subject	Pre	T 1	T 2	Post
5	23.89	23.30	24.25	22.32
6	36.67	35.85	33.97	40.51
7	32.07	28.80	26.39	25.94
8	32.56	35.82	35.99	32.66

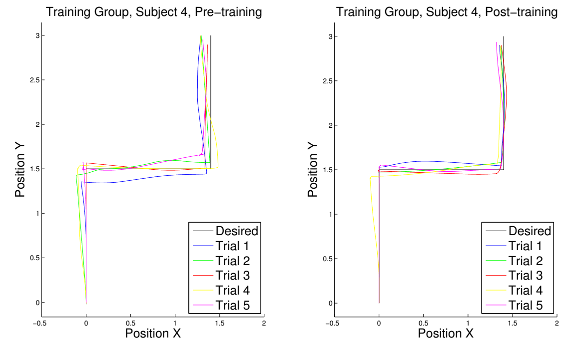

(a) Subject 4, FF group

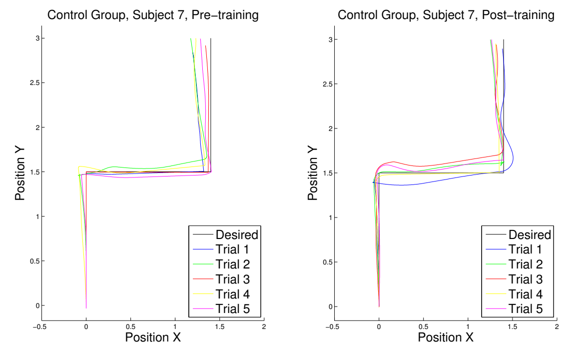

(b) Subject 7, Control group

Fig. 8. Comparison between the Pre- and Post-training of two typical subjects in the Training group and Control group.

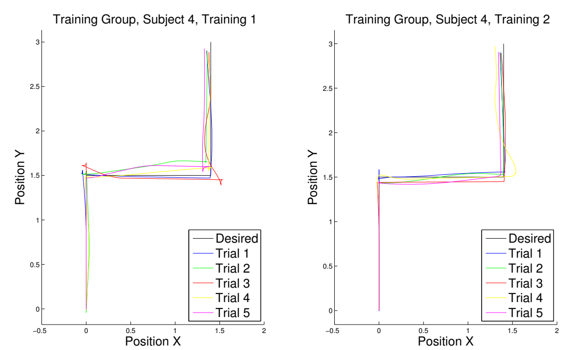

Fig. 9. Two training sessions of Subject 4 in Training group.

IV. INFANT DRIVING EXPERIMENTS

The experiments were carried out with two developmentally challenged infants - a 2-year old with spina bifida and a 3-year old with cerebral palsy, using an institution approved protocol. The infant with spina bifida had good control of his hand movement but lacked the ability to walk and balance himself, while the infant with cerebral palsy had decreased control of hand movement and coordination.

Each training consisted of 4 sessions, similar to adult experiments. Each session had 2 trials. The training was repeated for 5 non-consecutive days. A trainer stood at a turning point on the path and moved on to the next turning point or the goal once the infant reached this point. This was repeated over all sessions and trials.

Tables V and VII list the deviation area between the desired and the actual paths for the two infants. Tables VI and VIII show the travel time data.

TABLE V
DEVIATION AREA (m^2) OF INFANT 1

Day	Session	Trial 1	Trial 2	Average	Decrease
1	Pre	2.2499	2.2904	2.2702	54.92%
	Training1	1.2151	1.3468	1.2810	
	Training2	0.5638	0.9997	0.7818	
	Post	1.4253	0.6213	1.0233	
2	Pre	2.2671	2.0992	2.1832	29.57%
	Training1	0.8011	1.3815	1.0913	
	Training2	0.5924	0.5160	0.5542	
	Post	1.5648	1.5103	1.5376	
3	Pre	1.2745	0.7874	1.0310	6.51%
	Training1	0.6019	0.3503	0.4761	
	Training2	0.4161	0.6740	0.5451	
	Post	1.1309	0.7967	0.9638	
4	Pre	0.5628	0.3598	0.4613	13.39%
	Training1	0.8273	0.4511	0.6392	
	Training2	0.2507	0.2806	0.2657	
	Post	0.3841	0.4150	0.3996	
5	Pre	0.3491	0.4203	0.3847	0.79%
	Training1	0.3784	0.2483	0.3134	
	Training2	0.2466	0.3154	0.2810	
	Post	0.3979	0.3654	0.3817	

TABLE VI
AVERAGE TRAVEL TIME ($second$) OF INFANT 1

Day	Pre	Training 1	Training 2	Post
1	21.86	44.32	44.31	32.92
2	83.86	35.99	30.81	79.86
3	28.04	40.80	44.88	39.52
4	23.97	26.22	21.66	45.72
5	24.12	23.68	21.96	24.87

The following observations can be made from our pilot data:

1) The deviation area from the desired path consistently decreased during the five days of training (Fig. 10). In the beginning of training, the infants do not turn or follow the path. By day 4 and 5 of the training, the performance during Pre- or Post-training has significant improvements.
2) When the force field is turned on, the babies track the path much better, as shown in Fig. 12. Both babies' tracking error are much lower than the Pre-training session (Fig. 11) and Post-training session of the same day (Day 1).
3) From the data on travel time, one observes that there is no built in pattern. One reason is that babies sometimes stop and stare around in the environment once they see or hear interesting things.

V. CONCLUSION

In this paper, we presented a novel strategy to train infant drivers to make turns with mobile robots using force field

TABLE VII
DEVIATION AREA (m^2) OF INFANT 2

Day	Session	Trial 1	Trial 2	Average	Decrease
1	Pre	2.2885	1.7552	2.0219	42.74%
	Training1	0.5782	0.3847	0.4815	
	Training2	0.3304	0.4519	0.3912	
	Post	1.3922	0.9232	1.1577	
2	Pre	1.0617	1.1784	1.1201	24.55%
	Training1	0.4985	0.6478	0.5732	
	Training2	0.2385	0.3989	0.3187	
	Post	0.6804	1.0097	0.8451	
3	Pre	0.9346	0.6811	0.8079	31.60%
	Training1	0.3102	0.2154	0.2628	
	Training2	0.3014	0.2975	0.2995	
	Post	0.6690	0.4361	0.5526	
4	Pre	0.4649	0.2885	0.3767	9.58%
	Training1	0.1371	0.1831	0.1601	
	Training2	0.2289	0.1677	0.1983	
	Post	0.2783	0.4029	0.3406	
5	Pre	0.3985	0.2693	0.3339	1.32%
	Training1	0.2627	0.2699	0.2663	
	Training2	0.1526	0.1540	0.1533	
	Post	0.3761	0.2829	0.3295	

TABLE VIII
AVERAGE TRAVEL TIME ($second$) OF INFANT 2

Day	Pre	Training 1	Training 2	Post
1	54.95	34.80	44.39	213.95
2	181.71	105.40	125.28	169.24
3	91.92	68.58	45.79	59.27
4	68.44	68.37	92.55	71.41
5	66.23	76.40	56.91	71.88

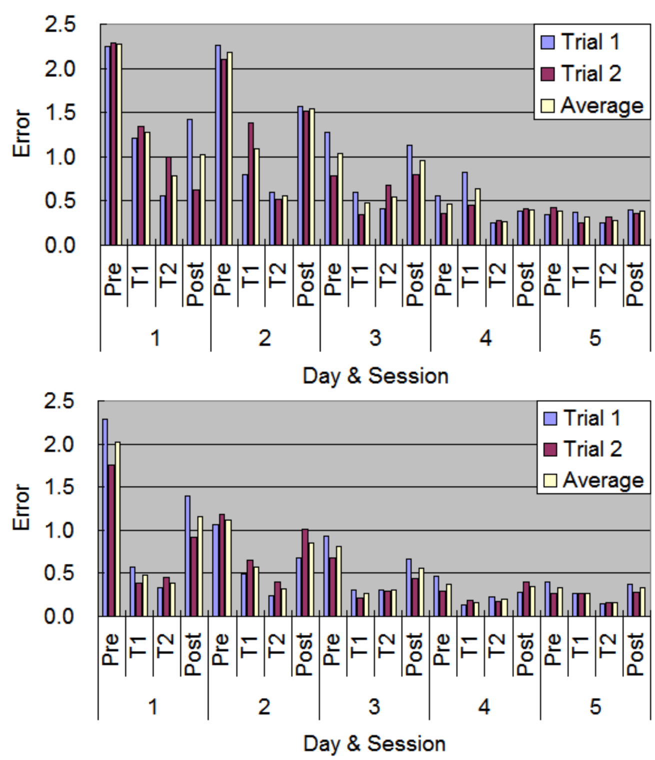

Fig. 10. Error from the desired path over 5 Days of training for (i) Infant 1, (ii) Infant 2. Note that there are four data collecting sessions each day that include Pre-training, two training sessions with the force field, and one Post-training. The deviation area from the desired path decreases continuously over the days for Pre-training or Post-training data. Note that on a particular day, the training helps lower this deviation but eventually plateaus by the end of 5th day.

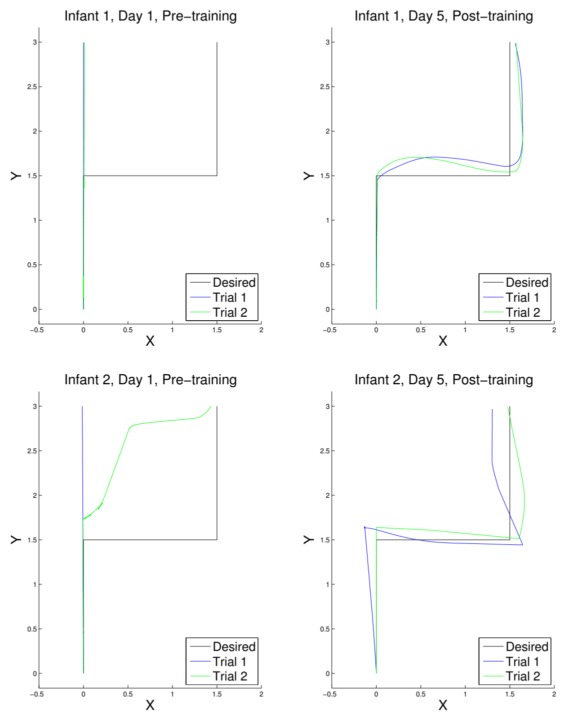

Fig. 11. Pre-training data on Day 1 and Post-training data on Day 5 - both without force fields (i) Infant 1, (ii) Infant 2.

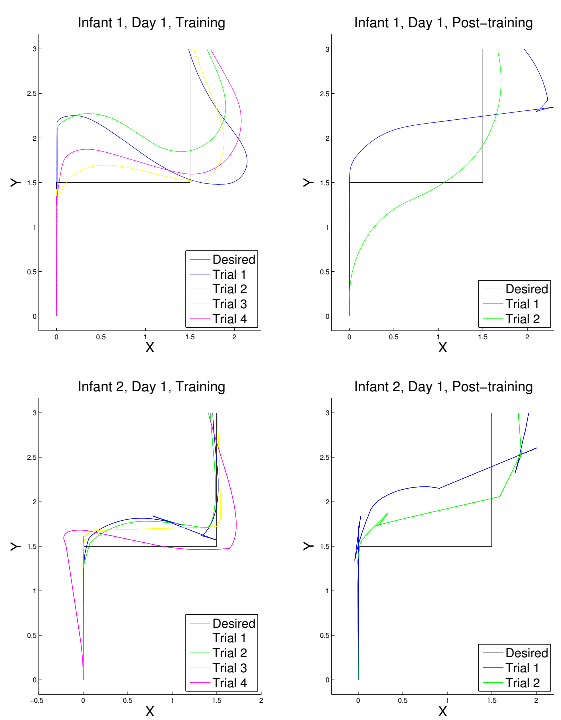

Fig. 12. Two Infants' Training and Post-training data on Day 1.

joystick and an 'assist-as-needed' paradigm. Experiments were conducted with two developmentally challenged infant drivers, one with spina bifida and the other with cerebral palsy. Pre-training data for the infant drivers on day 1 showed complete inability to follow a desired path with turns. Pre-training and post-training data on day 5, in the absence of force field, showed that the infants had learnt to control the joystick to move the robot in different directions. Additionally, the learning became progressively better over the 5 days of training for both infants. In future, we plan to extend this methodology to train babies to avoid obstacles as well as learn complex social behaviors such as interacting with peers.

VI. Acknowledgments

The authors gratefully acknowledge Christina Ragonesi and Terri Peffley for help during infant experimentation.

References

[1] Campos, J.J., Anderson, D.I., Barbu-Roth, M.A., Hubbard, E.M., Hertenstein, M.J., Witherington, D., *Travel Broadens the Mind*, Infancy, 1(2):149-219, 2000.

[2] Anderson, D.I., Campos, J.J., Anderson, D.E., Thomas, T.D., Witherington, D.C., Uchiyama, I., Barbru-Roth, M.A., *The flip side of perception-action coupling: locomotor experience and the ontogeny of visual-postural coupling*, Human Movement Science, Vol. 20, No. 4-5. (2001), pp. 461-487.

[3] Teft, D., Guerette, P., Furumasu, J., *Cognitive predictors of young children's readiness for powered mobility*, Dev Med Child Neurol. 1999 Oct;41(10):665-70.

[4] Galloway, J.C., Ryu, J.C., Agrawal, S.K., *Babies driving robots: self-generated mobility in very young infants*, Intel Serv Robotics 1:123C134, 2008.

[5] Lynch, A., Ryu, J.C., Agrawal, S.K., Galloway, J.C., *Power Mobility Training for a 7-month-old Infant with Spina Bifida*, Pediatric Physical Therapy, Vol. 24, No. 4, 2009, 362-368.

[6] Banala, S.K., Kim, S.H., Agrawal, S.K., Scholz, J.P., *Robot Assisted Gait Training with Active Leg Exoskeleton (ALEX)*, IEEE Transactions on Neural Systems and Rehabilitation Engineering, Vol. 17, No. 1, 2009, 2-8.

[7] Kim, S.H., Banala, S.K., Agrawal, S.K., Krishnamoorthy, V., Scholz, J.P., *Robot-assisted Gait Training Aids Adaptation in Healthy Individuals*, Experimental Brain Research, 2010, to appear.

[8] Han, S., Lee, J., *Tele-operation of a Mobile Robot Using a Force Reflection Joystick with a Single Hall Sensor*, 16th IEEE Inter. Conf. on Robot & Human Interactive Communication, Aug. 2007.

[9] Wang, X., Seet, G.G.L., Lau, M.W.S., Low, E., Tan, K.C., *Exploiting Force Feedback in Pilot Training and Control of an Underwater Robotics Vehicle: an Implementation in LabVIEW*, OCEANS 2000 MTS/IEEE Conference and Exhibition, Vol. 3, (2000), pp. 2037-2042.

[10] Rubio-Sierra, F.J., Stark, R.W., Thalhammer, S., Heckl, W.M., *Force-feedback Joystick as a Low-cost Haptic Interface for an Atomic-force-microscopy nanomanipulator*, Appl. Phys. A 76, 903-906, 2003.

[11] Luo, R.C., Hu, C.Y., Chen, T.M., Lin, M.H., *Force Reflective Feedback Control for Intelligent Wheelchairs*, Proc. of the 1999 IEEE/RSJ Intl. Conf. on Intelligent Robots and Systems, 1999.

[12] Lee, S., Sukhatme, G.S., Kim, G.J., Park, C.M., *Haptic Control of a Mobile Robot: A User Study*, Proc. of the 2002 IEEE/RSJ Intl. Conf. on Intelligent Robots and Systems, Oct. 2002.

[13] Fattouh, A., Sahnoun, M., Bourhis, G., *Force Feedback Joystick Control of a Powered Wheelchair: Preliminary Study*, IEEE International Conference on Systems, Man and Cybernetics, 2004.

[14] Bourhis, G., Sahnoun, M., *Assisted Control Mode for a Smart Wheelchair*, Proc. of the 2007 IEEE 10th Intl. Conf. on Rehabilitation Robotics, June 12-15.

[15] Bemporad, A., Di Marco, M., Tesi, A., *Wall-Following Controllers for Sonar-Based Mobile Robots*, IEEE International Conference on Systems, Man and Cybernetics, 2004.